Milliarcsecond Imaging of the Radio Emission from the Quasar with the Most Massive Black Hole at Reionization

The Astrophysical Journal Letters, 835:L20 (4pp), 2017 February 1 doi:10.3847/2041-8213/835/2/L20

Milliarcsecond Imaging of the Radio Emission from the Quasar with the Most Massive Black Hole at Reionization

Ran Wang[1], Emmanuel Momjian[2], Chris L. Carilli[2], Xue-Bing Wu[1,3], Xiaohui Fan[4], Fabian Walter[5], Michael A. Strauss[6], Feige Wang[3], and Linhua Jiang[1]
[1] Kavli Institute of Astronomy and Astrophysics at Peking University, No. 5 Yiheyuan Road, Haidian District, Beijing 100871, China
[2] National Radio Astronomy Observatory, P.O. Box 0, Socorro, NM 87801, USA
[3] Department of Astronomy, School of Physics, Peking University, No. 5 Yiheyuan Road, Haidian District, Beijing 100871, China
[4] Steward Observatory, University of Arizona, 933 N Cherry Avenue, Tucson, AZ 85721, USA
[5] Max-Planck-Institute for Astronomy, Königsstuhl 17, D-69117 Heidelberg, Germany
[6] Department of Astrophysical Sciences, Princeton University, Princeton, NJ 08544, USA
Received 2016 December 5; revised 2017 January 5; accepted 2017 January 7; published 2017 January 25

Abstract

We report Very Long Baseline Array (VLBA) observations of the 1.5 GHz radio continuum emission of the $z = 6.326$ quasar SDSS J010013.02+280225.8 (hereafter J0100+2802). J0100+2802 is by far the most optically luminous and is a radio-quiet quasar with the most massive black hole known at $z > 6$. The VLBA observations have a synthesized beam size of 12.10 mas ×5.36 mas (FWHM), and detected the radio continuum emission from this object with a peak surface brightness of 64.6 ± 9.0 μJy beam^{-1} and a total flux density of 88 ± 19 μJy. The position of the radio peak is consistent with that from SDSS in the optical and *Chandra* in the X-ray. The radio source is marginally resolved by the VLBA observations. A 2D Gaussian fit to the image constrains the source size to (7.1 ± 3.5) mas × (3.1 ± 1.7) mas. This corresponds to a physical scale of (40 ± 20) pc × (18 ± 10) pc. We estimate the intrinsic brightness temperature of the VLBA source to be $T_{\rm B} = (1.6 \pm 1.2) \times 10^7$ K. This is significantly higher than the maximum value in normal star-forming galaxies, indicating an active galactic nucleus (AGN) origin for the radio continuum emission. However, it is also significantly lower than the brightness temperatures found in highest-redshift radio-loud quasars. J0100+2802 provides a unique example for studying the radio activity in optically luminous and radio-quiet AGNs in the early universe. Further observations at multiple radio frequencies will accurately measure the spectral index and address the dominant radiation mechanism of the radio emission.

Key words: galaxies: active – galaxies: high-redshift – quasars: individual (SDSS J010013.02+280225.8) – radio continuum: galaxies

1. Introduction

The large sample of quasars that have been discovered at $z \geqslant 6$ gives us the best opportunity to study the formation of the first supermassive black holes (SMBHs) at the epoch of cosmic reionization (e.g., Fan et al. 2006; Willott et al. 2010; Mortlock et al. 2011; Jiang et al. 2015; Venemans et al. 2015; Bañados et al. 2016; Matsuoka et al. 2016). Observations from X-ray to radio wavelengths indicate that the broadband spectral energy distributions of most of these earliest quasars are comparable to those of the optically selected quasars at low-z (Jiang et al. 2006). However, their average Eddington ratio (the ratio between the quasar bolometric luminosity and Eddington luminosity) is close to unity (Willott et al. 2010; De Rosa et al. 2011, 2014). This is higher than the average value of 0.16 found with the luminosity-matched low-z SDSS quasar sample (De Rosa et al. 2011), indicating that the SMBHs are accreting close to the Eddington limit in these young quasars at the earliest epoch.

Radio observations of the optically selected $z > 5.5$ quasars with the Very Large Array (VLA) at 1.4 GHz, including data from the Faint Images of the Radio Sky at Twenty-Centimeters (Becker et al. 1995), yield a radio-loud fraction of $8.1^{+5.0}_{-3.2}$%, which is comparable to the radio-loud fraction found with samples of low-z optical quasars (Jiang et al. 2007; Bañados et al. 2015). Four of the radio-loud quasars at $z > 5.7$ (SDSS J0836+0054, Frey et al. 2003, 2005; SDSS J1427+3312, Frey et al. 2008; Momjian et al. 2008; CFHQS J1429+5447, Frey et al. 2011; SDSS J2228+0110, Cao et al. 2014) were observed using the Very Long Baseline Interferometry (VLBI) with the European VLBI Network (EVN) and/or the Very Long Baseline Array (VLBA) at ⩽10 mas resolution at multiple frequencies. The VLBI images reveal compact radio emission on scales of a few tens of parsecs and steep radio spectra ($S_\nu \sim \nu^\alpha$) with spectral indices of $\alpha = -0.8 \sim -1.1$ (Frey et al. 2005, 2008, 2011; Momjian et al. 2008). The EVN and VLBA images of SDSS J1427+3312 resolved the radio emission into two components separated by about 170 pc, indicating a very young symmetric radio structure with possible kinematic age of only 10^3 years (Frey et al. 2008; Momjian et al. 2008).

In this Letter, we report VLBA observations of a radio-quiet quasar, SDSS J010013.02+280225.8 (hereafter J0100+2802) at $z = 6.326$ (Wu et al. 2015; Wang et al. 2016). J0100+2802 is the most optically luminous quasar discovered at $z > 6$, which hosts the most massive SMBH of $M_{\rm BH} \approx 1.2 \times 10^{10}\, M_\odot$ among the known $z > 6$ quasars (Wu et al. 2015). The X-ray to near-infrared observations yield a quasar bolometric luminosity close to the Eddington luminosity (Wu et al. 2015; Ai et al. 2016), suggesting that we are witnessing the rapid accretion of this very massive SMBH. Our VLA observations at 3 GHz detected the radio continuum from this object with an observed flux density of $S_{3\,\rm GHz} = 104.5 \pm 3.1$ μJy. The radio and optical data estimate the radio loudness of this object to be $R = f_{\nu,5\,\rm GHz}/f_{\nu,4400\,\text{Å}} = 0.9$ for a steep radio spectrum ($S_\nu \sim \nu^{-0.9}$) or $R = 0.2$ for a flat spectrum

($S_\nu \sim \nu^{-0.06}$; see the discussion in Wang et al. 2016). This indicates that the central AGN is radio quiet[7] but not radio silent. J0100+2802 is the best example for studying the radio activity from optically luminous but radio-quiet quasars at the earliest epoch.

The VLBA observations presented in this Letter provide the first 10 mas resolution (~60 pc at the quasar redshift) image of a radio-quiet quasar at the highest redshift, which allows us to constrain the source size and brightness temperature of the radio emission from this powerful AGN in the early universe. The observation and data reduction are described in Section 2, the results are presented and discussed in Section 3, and the main conclusions are summarized in Section 4. We adopt a ΛCDM cosmology with $H_0 = 71$ km s^{-1} Mpc^{-1}, $\Omega_M = 0.27$, and $\Omega_\Lambda = 0.73$ throughout this paper (Spergel et al. 2007).

2. Observations and Data Reduction

We observed the 1.5 GHz radio continuum emission from J0100+2802 using the VLBA. The observations were carried out in 2016 February and March in eight separate observing sessions. The data at each VLBA station were recorded using the Roach Digital Backend and the polyphase filterbank digital signal-processing algorithm (PFB) with sixteen 32 MHz data channels. This provided eight contiguous 32 MHz data channels at matching frequencies in each of the two circular polarizations. The data were sampled at two bits. We employed nodding-style phase-referencing with a cycle time of 5 minutes: 4 minutes on the target and 1 minute on the phase calibrator, J0057+3021, which is 2.°4 away from the target. The source 3C 84 was observed as a fringe finder and bandpass calibrator. The total observing time was 22 hr, and the total on target-source time was 16 hr. We used the VLBA DiFX correlator (Deller et al. 2011) in Socorro, NM, with an integration time of 2s. Each 32 MHz data channel was further split into 128 spectral points.

We edited and calibrated the data using the Astronomical Image Processing System (AIPS; Greisen 2003) following standard VLBI data reduction procedures. We then performed self-calibration on the phase calibrator and applied the solution to the target. The continuum emission from the target was then imaged adopting natural weighting. The resulting synthesized beam size (FWHM) of the final image is 12.10 mas × 5.36 mas, or 68.5 pc × 30.3 pc at the quasar redshift of $z = 6.326$. We also tapered the visibility data using a Gaussian function that falls to 30% at 5 Mλ in both the u and v directions to obtain a lower-resolution image and recover more flux density in the extended area. We list the observing parameters and the 1σ rms noise values of both the full resolution and tapered images in Table 1.

3. Results and Discussion

We detect radio continuum emission with a single peak from the VLBA 1.5 GHz image of the quasar J0100+2802. The observing frequency of 1.5 GHz corresponds to a rest-frame frequency of 11 GHz at the quasar redshift of $z = 6.326$ (Wang et al. 2016). We list the peak surface brightness and the peak position of the VLBA source, as well as other measurements in Table 1. Considering the synthesized beam, signal-to-noise ratio, positional uncertainty of the phase-reference calibrator, and the angular distance between the reference calibrator and the target, the position accuracy of this measurement is ~1 mas (Reid & Honma 2014). The VLBA peak position is about 16 mas away from the peak position (R.A. = $01^h00^m13^s.024$, decl. = $+28^d02'25''.80$) of the previous VLA 3 GHz detection (Wang et al. 2016). Note that the thermal noise introduces a position error of $0.5\mathrm{FWHM}_{\mathrm{beam}}/\mathrm{SNR} \sim 10$ mas (Reid &

[7] We here adopt $R = f_{\nu,5\,\mathrm{GHz}}/f_{\nu,4400\,\text{Å}} = 10$ to separate radio-loud and radio-quiet quasars (Kellermann et al. 1989).

Table 1
VLBA Observation of J0100+2802

Total observing time (hr)	22
Observing frequency (GHz)	1.5
Total bandwidth (MHz)	256
Phase calibrator	J0057+3021
Full resolution image of J0100+2802:	
FWHM beam size (mas)	12.10 × 5.36[a]
Beam P.A. (°)	5
Image 1σ rms sensitivity (μJy beam^{-1})	9
Peak position (J2000)	01:00:13.0250+28:02:25.791
Peak surface brightness (μJy beam^{-1})	64.6 ± 9.0
Total flux density (μJy)	88 ± 19.0
Deconvolved FWHM source size (mas)	(7.1 ± 3.5) × (3.1 ± 1.7)
P.A. (°)	170 ± 14
Brightness temperature (K)	(1.6 ± 1.2) × 10^7
Tapered image of J0100+2802:	
FWHM beam size (mas)	34.1 × 28.3[a]
Beam P.A. (°)	32
Image 1σ rms sensitivity (μJy beam^{-1})	17
Total flux density (μJy)	91 ± 17

Note.
[a] Natural weighting.

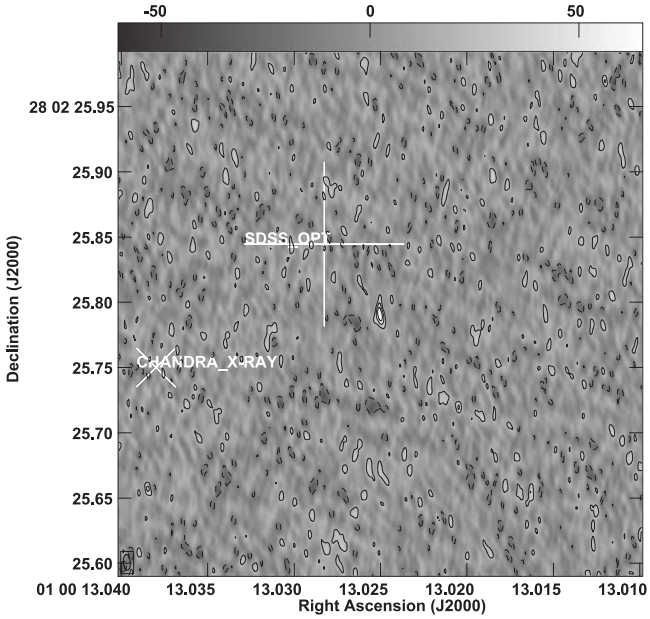

Figure 1. Radio emission from J0100+2802 detected by the VLBA at 1.5 GHz, compared to the positions of the quasar measured from SDSS in the optical and *Chandra* in X-ray band. The image is centered on the peak position of the VLBA detection, and the contours are [−2, 2, 4, 6] × 9 μJy beam^{-1}. The step-wedge at the top of the image shows the grayscale in units of μJy beam^{-1}. The white plus sign represents the position and uncertainties (~0.″06) in R.A. and decl. from SDSS. The cross shows the X-ray source position detected by *Chandra* (Ai et al. 2016). The *Chandra* observation has a position uncertainty of 0.″6 (Ai et al. 2016), which is larger than the field of view of 0.″4 × 0.″4 shown here. The synthesized beam is plotted at the bottom left of the image

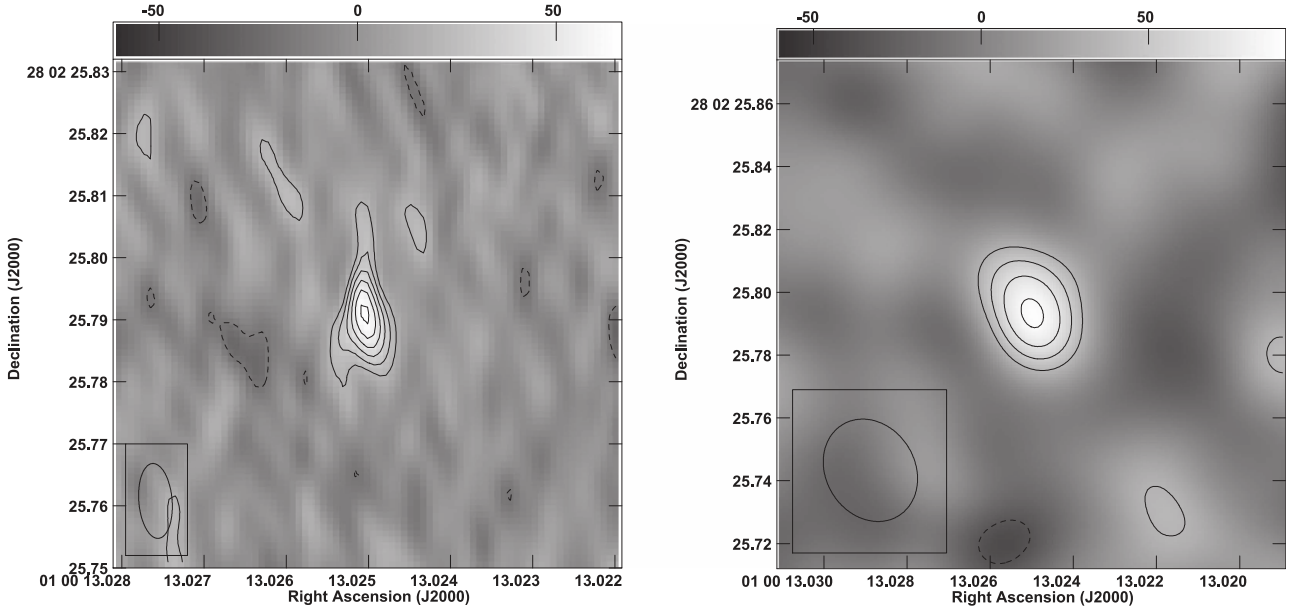

Figure 2. Left: the full resolution 1.5 GHz image of J0100+2802 (the same as Figure 1), zooming in to a smaller field of view of $0\farcs08 \times 0\farcs08$ to show the radio source detected by the VLBA. The contours are $[-3, -2, 2, 3, 4, 5, 6, 7] \times 9$ μJy beam^{-1}. Right: image made by the visibility data tapered at 5 Mλ. The contours are $[-2, 2, 3, 4, 5] \times 17$ μJy beam^{-1}, and the synthesized beam is shown at the bottom left. The step-wedges at the tops of both images show the grayscale in units of μJy beam^{-1}. The elliptics on the bottom left of each image show the FWHM beam sizes of the full resolution and the tapered images (see Table 1). Natural weighting is adopted for both images.

Honma 2014) in the VLA measurement, and the calibrator of the VLA observations also has an position uncertainty[8] that can range between 10 and 150 mas. Thus, the source position from the VLBA observations is in agreement with the VLA 3 GHz data within the expected errors. Figure 1 compares the position to those measured by the Sloan Digital Sky Survey in the optical and the *Chandra* X-ray telescope (Wu et al. 2015; Ai et al. 2016; Wang et al. 2016). The VLBA peak is within the astrometric errors of the optical and X-ray observations.

The radio emission is marginally resolved by the VLBA (left panel of Figure 2). We performed 2D Gaussian fitting to the VLBA image using the IMFIT task in the Common Astronomy Software Applications package (McMullin et al. 2007). The deconvolved FWHM source size (see Table 1) corresponds to a physical scale of (40 ± 20) pc $\times$ (18 ± 10) pc, i.e., $\sim 3.4 \times 10^4$ Schwarzschild radii, at the quasar redshift. The total source flux density from the Gaussian fit is 88 ± 19 μJy. In order to better recover the total flux density of this radio component, we tapered the visibility data at 5 Mλ. The tapered image shows an unresolved source with a peak flux density of 91 ± 17 μJy, which is consistent with the total flux density measured with the full resolution image (right panel of Figure 2). Based on the total 1.5 GHz flux density and the deconvolved source size from the full resolution image, we derived the intrinsic brightness temperature to be $T_{\rm B} = (1.6 \pm 1.2) \times 10^7$ K. This is more than two orders of magnitude higher than the maximum brightness temperature in normal star-forming galaxies (i.e., $T_{\rm B} \leqslant 10^5$ K at $\nu \geqslant 1$ GHz, Condon 1992), indicating an AGN origin for the radio emission. However, this brightness temperature is significantly lower than the values of $\sim 10^8$–10^9 K found for the radio-loud quasars at $z \sim 6$ at a similar frequency (Momjian et al. 2008; Frey et al. 2011; Cao et al. 2014).

[8] The calibrator J0119+321 is in the C Category of position accuracy according to https://science.nrao.edu/facilities/vla/observing/callist.

There are no low-resolution observations of this quasar at 1.5 GHz. The flux density not included in the VLBA observations, if any, is unknown, and thus the spectral index of the radio continuum from 3 to 1.5 GHz (i.e., 22 to 11 GHz in the quasar rest-frame) is unknown. Our previous 3 and 32 GHz observations with the VLA suggest a steep power-law spectrum of $S_\nu \sim \nu^{-0.9 \pm 0.15}$ from rest-frame 234 to 22 GHz, while the flux densities measured in the observing frequency window of 2–4 GHz (around 22 GHz in the rest-frame) prefer a flat spectrum of $S_\nu \sim \nu^{-0.06 \pm 0.22}$ (Wang et al. 2016). The 1.5 GHz flux densities, derived with the 3 GHz data of $S_{\rm 3GHz} = 104.5 \pm 3.1$ μJy and the steep and flat spectra described above, are 195 ± 21 μJy and 109 ± 17 μJy, respectively.

The VLBA detection of 88 ± 19 μJy is lower, but marginally consistent with the flat spectral estimate. However, it is only 45% of the value in the steep spectrum case. If there is no more diffuse emission, i.e., the VLBA source dominates the 1.5 GHz radio emission from J0100+2802, the VLA and VLBA data may indicate a radio spectrum that is steep at 200–20 GHz and which flattens/turns over at 20–10 GHz. However, we notice that at the rest-frame frequency of 11 GHz, the brightness temperature of 1.6×10^7 K is too low for radio emission turnover produced by synchrotron self absorption (Gallimore et al. 1996). Low brightness temperatures of 10^6 to 10^7 K and flat/turnover spectra have been discovered in VLBA imaging of low-z AGNs (Gallimore et al. 2004; Krips et al. 2007), which may be explained as free–free or synchrotron emission from an X-ray heated corona or disk wind (Krips et al. 2006; Blundell & Kuncic 2007; Raginski & Laor 2016). Further observations at multiple frequencies are needed to properly measure the radio spectral index in the 1–100 GHz frequency range, determining whether the radio spectrum of J0100+2802 is similar to the steep spectra found with the radio-loud objects, or if it flattens toward centimeter wavelengths. These, together with the VLBA image will finally constrain the radiation mechanism of the radio emission from

this extremely luminous and radio-quiet quasar at the highest redshift.

4. Conclusions

We presented VLBA 1.5 GHz observations of the radio continuum emission from the radio-quiet quasar J0100+2802 at $z = 6.326$. The VLBA observation reveals a compact radio source on scales of $\sim 40 \pm 20$ pc, with a total flux density of $88 \pm 19\ \mu$Jy (see Table 1). This is much lower than the flux density derived from a steep power-low spectrum of $S_\nu \sim \nu^{-0.9}$ based on previous VLA 3 and 32 GHz observations. This is the first time the radio emission from a radio-quiet quasar at $z > 6$ has been imaged with the VLBA. The peak position of the VLBA source is within the uncertainties of the quasar locations measured by SDSS in the optical and *Chandra* in the X-ray; no clear offset is detected between the radio emission and the optically luminous AGN. We estimate the brightness temperature of the VLBA source to be $(1.6 \pm 1.2) \times 10^7$ K. This is much higher than maximum values of normal star-forming galaxies, indicating that radio activity from the central AGN is the dominant source of the VLBA detection. J0100+2802 provides a unique example for further radio observations at multiple frequencies and a detailed study of the radiation mechanism of the young and radio-quiet quasars at the highest redshift.

The data presented in this Letter are based on observations of VLBA project 16A-247. The National Radio Astronomy Observatory is a facility of the National Science Foundation operated under cooperative agreement by Associated Universities, Inc. This work made use of the Swinburne University of Technology software correlator, developed as part of the Australian Major National Research Facilities Programme and operated under licence. We are thankful for the supports from the National Science Foundation of China (NSFC) grant Nos.11373008, 11533001, the Strategic Priority Research Program "The Emergence of Cosmological Structures" of the Chinese Academy of Sciences, grant No. XDB09000000, the National Key Basic Research Program of China 2014CB845700. This work was supported by National Key Program for Science and Technology Research and Development (grant 2016YFA0400703). R.W. acknowledge supports from the Thousand Youth Talents Program of China, the NSFC grant Nos. 11443002 and 11473004. X.F. acknowledge supports from NSF grants AST 11-07682 and 15-15115.

Facility: VLBA.

References

Ai, Y., Dou, L., Fan, X., et al. 2016, ApJL, 823, L37
Bañados, E., Venemans, B. P., Decarli, R., et al. 2016, ApJS, 227, 11
Bañados, E., Venemans, B. P., Morganson, E., et al. 2015, ApJ, 804, 118
Becker, R. H., White, R. L., & Helfand, D. J. 1995, ApJ, 450, 559
Blundell, K. M., & Kuncic, Z. 2007, ApJL, 668, L103
Cao, H.-M., Frey, S., Gurvits, L. I., et al. 2014, A&A, 563, 111
Condon, J. J. 1992, ARA&A, 30, 575
Deller, A. T., Brisken, W. F., Phillips, C. J., et al. 2011, PASP, 123, 275
De Rosa, G., Decarli, R., Walter, F., et al. 2011, ApJ, 739, 56
De Rosa, G., Venemans, B. P., Decarli, R., et al. 2014, ApJ, 790, 145
Fan, X., Strauss, M. A., Richards, G. T., et al. 2006, AJ, 131, 1203
Frey, S., Gurvits, L. I., Paragi, Z., & Gabányi, K. É. 2008, A&A, 484, L39
Frey, S., Mosoni, L., Paragi, Z., & Gurvits, L. I. 2003, MNRAS, 343, 20
Frey, S., Paragi, Z., Gurvits, L. I., Gabányi, K. É., & Cseh, D. 2011, A&A, 531, L5
Frey, S., Paragi, Z., Mosoni, L., & Gurvits, L. I. 2005, A&A, 436, L13
Gallimore, Jack F., Baum, S. A., & O'Dea, C. P. 2004, ApJ, 613, 794
Gallimore, J. F., Baum, S. A., O'Dea, C. P., & Pedlar, A. 1996, ApJ, 458, 136
Greisen, E. W. 2003, in Information Handling in Astronomy—Historical Vistas, Astrophysics and Space Science Library, Vol. 285 (Dordrecht: Kluwer), 109
Jiang, L., Fan, X., Hines, D. C., et al. 2006, AJ, 132, 2127
Jiang, L., Fan, X., Ivezić, Ż., et al. 2007, ApJ, 656, 680
Jiang, L., McGreer, I. D., Fan, X., et al. 2015, AJ, 149, 188
Kellermann, K. I., Sramek, R., Schmidt, M., Shaer, D. B., & Green, R. 1989, AJ, 98, 1195
Krips, M., Eckart, A., & Krichbaum, T. P. 2007, A&A, 464, 553
Krips, M., Eckart, A., Neri, R., et al. 2006, A&A, 446, 113
Matsuoka, Y., Onoue, M., Kashikawa, N., et al. 2016, ApJ, 828, 26
McMullin, J. P., Waters, B., Schiebel, D., Young, W., & Golap, K. 2007, in ASP Conf. Ser. 376, Astronomical Data Analysis Software and Systems XVI, ed. R. A. Shaw, F. Hill, & D. J. Bell (San Francisco, CA: ASP), 127
Momjian, E., Carilli, C. L., & McGreer, I. D. 2008, AJ, 136, 344
Mortlock, D. J., Warren, S. J., Venemans, B. P., et al. 2011, Natur, 474, 616
Raginski, I., & Laor, A. 2016, MNRAS, 459, 2082
Reid, M. J., & Honma, M. 2014, ARA&A, 52, 339
Spergel, D. N., Bean, R., Doré, O., et al. 2007, ApJS, 170, 377
Venemans, B. P., Bañados, E., Decarli, R., et al. 2015, ApJL, 801, L11
Wang, R., Wu, X.-B., Neri, R., et al. 2016, ApJ, 830, 53
Willott, C. J., Delorme, P., Reylé, C., et al. 2010, AJ, 139, 906
Wu, X.-B., Wang, F., Fan, X., et al. 2015, Natur, 518, 512